Aminobacter aminovorans NADH:Flavin Oxidoreductase His140: A Highly Conserved Residue Critical for NADH Binding and Utilization†

Thomas R. Russell‡ and Shiao-Chun Tu*,‡,§

Departments of Biology and Biochemistry and Chemistry, University of Houston, Houston, Texas 77204-5001

Received July 14, 2004

ABSTRACT: Homodimeric FRD_{Aa} Class I is an NADH:flavin oxidoreductase from *Aminobacter aminovorans*. It is unusual because it contains an FMN cofactor but utilizes a sequential-ordered kinetic mechanism. Because little is known about NADH-specific flavin reductases in general and FRD_{Aa} in particular, this study aimed to further explore FRD_{Aa} by identifying the functionalities of a key residue. A sequence alignment of FRD_{Aa} with several known and hypothetical flavoproteins in the same subfamily reveals within the flavin reductase active-site domain a conserved GDH motif, which is believed to be responsible for the enzyme and NADH interaction. Mutation of the His140 in this GDH motif to alanine reduced FRD_{Aa} activity to <3%. An ultrafiltration assay and fluorescence quenching demonstrated that H140A FRD_{Aa} binds FMN in the same 1:1 stoichiometric ratio as the wild-type enzyme, but with slightly weakened affinity ($K_d = 0.9\ \mu$M). Anaerobic stopped-flow studies were carried out using both the native and mutated FRD_{Aa}. Similar to the native enzyme, H140A FRD_{Aa} was also able to reduce the FMN cofactor by NADH although much less efficiently. Kinetic analysis of anaerobic reduction measurements indicated that the His140 residue of FRD_{Aa} was essential to NADH binding, as well as important for the reduction of the FMN cofactor. For the native enzyme, the cofactor reduction was followed by at least one slower step in the catalytic pathway.

A Basic Local Alignment Search Tool−Protein (BLASTP)[1] search reveals that the number of putative and identified microbial two-component monooxygenases is growing rapidly as a result of ongoing genome-sequencing efforts. The constituents of two-component monooxygenases include the catalytically independent monofunctional flavin-dependent hydroxylase and NAD(P)H−flavin oxidoreductase (flavin reductase). The monofunctional flavin-dependent hydroxylases participate in catalyzing a bewildering and potentially useful array of reactions (*1*), including bioluminescence (*2*, *3*), synthesis of antibiotics such as actinorhodin (*4*, *5*), and bioremediation of harmful chemicals such as the herbicide 2,4,5-trichlorophenoxyacetate (*6*, *7*). Unlike bifunctional flavohydroxylases, which are able to catalyze the reduction and subsequent reoxidation of their own flavin prosthetic group (*1*), monofunctional flavin-dependent hydroxylases use reduced flavin as a cosubstrate. Flavin reductases provide reduced flavin to monofunctional flavin-dependent hydroxylases through the following reaction:

$$F + NAD(P)H + H^+ \rightarrow FH_2 + NAD(P)^+ \qquad (1)$$

where F is the oxidized flavin substrate and FH_2 is the reduced flavin product. F is most commonly FMN, but some enzymes also utilize riboflavin and FAD, and in some cases, they are the preferred substrates.

Flavin reductases specific for NADH and NADPH are named FRD and FRP, respectively, while general flavin reductases that use both pyridine nucleotides with similar efficiencies are named FRG. A subscript can be added to indicate from which organism the enzyme has been isolated. Class I enzymes have a flavin cofactor, while class II enzymes are nonflavoproteins. In general, these classes were distinguished not only by different amino acid sequences and folding motifs but also by kinetic mechanisms. However, in at least one case (*8*), an exception to such a general characterization has been recently noted.

FRP_{Vh} from *Vibrio harveyi* and FRG_{Vf} from *Vibrio fischeri* (both class I capable of providing reduced flavin to their respectively linked, light-producing monofunctional flavin-dependent hydroxylases, bacterial luciferase) have been extensively characterized as NADPH specific and NADPH−NADH general efficiency enzymes, respectively (*9*−*17*). Fre/FR class II from *Escherichia coli* has also been extensively

† Supported by Grant GM25953 from the National Institutes of Health and E-1030 from the Robert A. Welch Foundation.

* To whom correspondence should be addressed. Telephone: 713-743-8359. Fax: 713-743-8351. E-mail: dtu@uh.edu.
‡ Department of Biology and Biochemistry.
§ Department of Chemistry.

[1] Abbreviations: BLASTP, Basic Local Alignment Search Tool−Protein (http://www.ncbi.nlm.nih.gov/BLAST/); CD, circular dichroism; CDD, conserved domain database; DEAE cellulose and DEAE sepharose, diethylaminoethyl cellulose and diethylaminoethyl sepharose, respectively; FAD, flavin adenine dinucleotide; FMN and $FMNH_2$, oxidized and reduced riboflavin 5′-phosphate, respectively; FRD, NADH-preferring flavin reductase; FRG, NADH- and NADPH-utilizing general flavin reductase; FRP, NADPH-preferring flavin reductase; IPTG, isopropyl-β-D-thiogalactose; LB, Luria−Bertani; MWCO, molecular weight cut off; $NAD(P)^+$ and NAD(P)H, oxidized and reduced nicotinamide adenine dinucleotide and nicotinamide adenine dinucleotide phosphate, respectively; NCBI, National Center for Biotechnology Information; NmoA and NtaA, nitrilotriacetate monooxygenase component A; NmoB and NtaB, nitrilotriacetate monooxygenase component B; NTA, nitrilotriacetate; PDB, Protein Data Bank.

10.1021/bi048499n CCC: $27.50
Published on Web 09/14/2004

A

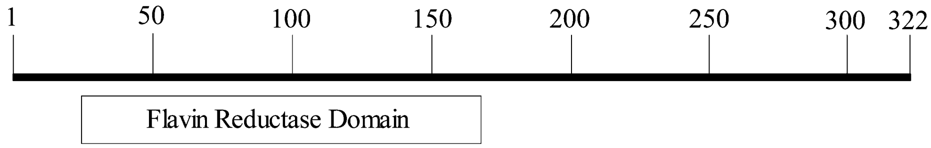

B

1	MGRLPTGGVYVVTAQD-CVPHGFTASSVSSVSLEPPLVMVCLAKTSRSHPALQESGRFAVNVLGEG-QKALARRFAK		
	RTRPEADRFAGVEWQTG-PTGCPVLEDALAYLECRVEQRVPV**GDH**TLVLGEVVAVGVLEE--GDPLALFHRRFGYTR	149	

C

FeR	88	.eKF.Gveyk........v.q.avA.Ie..V....D.**GTH**.l..G......l........	139
FRD_{Re}-II/DszD	117	..rFA..........G.Pvl.Gt.swm...V..l...**GDH**.lV.G.V..v..........	164
ActVB homolog	104	.DKFgG......E..G..v...aL..leC.V.a.H.a**GDH**.il.G.V..v.q........	154
FRD_{Sc}-I/ActVB	91	.DKFAG.ef..t...Ga.vldGavA.veCTV.....a**GDH**.il.G.VqSv..........	138
FRD_{Sp}-I/SnaC	100	.DrFAG.ef...d..G.P.l..a...l.C....V..a**GDH**.lV.G....i..........	148
Rv3567c	91	PDKFAGIDWRPSEL-GSPIIEGSLAYIDCTVASVHDG**GDH**FVVFGAVESLSEVPA-----	144
ActI/ORF6	100	PDKFAGIDW.PS.L.GSPIId.SLA.IDCTV.tVHDG**GDH**yVVFG.V.SmSEi.......	151
FRD_{Aa}-I/NmoB/NtaB	103	.DKFs.vDWh.....GaPlId.aLAY.DC...a.HeG**GDH**.im.G.V......g......	155
FRP_{Sv}-I/VlmR	109	...F..v.W......G.PvlE.aLA.l.C.l..l...**GAS**..l..A..............	151
FRD_{Ec}-II/HpaC	95	.erFs...W....L.a.Pvl.GSLA.le..i..V...**GTH**.V....i..i..........	142

FIGURE 1: Flavin reductase domain of FRD_{Aa} as the probable location of the active site. (A) Flavin reductase domain is located between residues 25−169 along the primary structure of FRD_{Aa}. (B) Consensus sequence of the flavin reductase domain as found in the CDD of NCBI. The putative pyridine nucleotide interaction motif (GDH) is underlined. (C) Partial sequence alignment of the flavin reductase domain of FRD_{Aa} with several known flavin reductases and hypothetical flavoproteins. The sequence from Rv3567c was selected by the alignment software as the reference; therefore, all of its residues are capitalized. Those residues from other sequences that have identity are also capitalized. Those residues from other sequences that are similar or have no identity or similarity are lowercase. The His140 residue of FRD_{Aa} (identified by the arrow) is well-conserved. FeR, ferric reductase complex with $NADP^+$ from *A. fulgidus*; FRD_{Re}-II/DszD, NADH:FMN oxidoreductase from *Rhodococcus erythropolis*; ActVB, homolog, from *Streptomyces roseofulvus*; FRD_{Sc}-I/ActVB, NADH:flavin oxidoreductase from *S. coelicolor*; FRD_{Sp}-I/SnaC, NADH:FMN oxidoreductase from *S. pristinaespiralis*; Rv3567c, hypothetical protein from *Mycobacterium tuberculosis* H37Rv; Act I/ORF 6, from *R. erythropolis*; FRD_{Aa}-I/NmoB/NtaB, NADH:flavin oxidoreductase from *A. aminovorans*; FRP_{Sv}-I/VlmR, NADPH:flavin oxidoreductase from *S. viridifaciens*; FRD_{Ec}-II/HpaC, NADH:flavin oxidoreductase from *E. coli*. An older but more comprehensive sequence alignment of this subfamily of flavin reductases as well as linked flavin-dependent hydroxylases can be found in Galán et al. (*23*).

characterized, but it has nonspecific substrate requirements (*18*, *19*). The NADH-specific enzymes lacked description for sometime and only recently have two NADH-specific enzymes been targeted for characterization (*8*, *20*). One of them, the NADH-specific FRD_{Aa} class I (formerly, NmoB or NtaB) has been isolated from *Aminobacter aminovorans* (formerly, *Chelatobacter heintzii*), a bacterium able to survive on the environmental contaminant NTA as its sole source of carbon, nitrogen, and energy, making it an effective bioremediation agent (*21*). FRD_{Aa} is believed to provide reduced flavin to NmoA (NtaA), a monofunctional flavin-dependent hydroxylase responsible for the initial degradation of NTA to iminodiacetate and glyoxylate through the following reaction:

$$Mg^{2+}{-}N(CH_2COO^-)_3 + FMNH_2 + O_2 \rightarrow HN(CH_2COO^-)_2 + H(CO)COO^- + FMN + H_2O + Mg^{2+} \quad (2)$$

FRD_{Aa} is a homodimer with a monomer molecular mass of 34.5 kDa, which undergoes a monomer−dimer equilibrium (*8*). This might have functional implications for NmoA, because both FRP_{Vh} and FRG_{Vf} undergo monomer−dimer equilibria as well, and it is known that this is at least one mechanism by which FRP_{Vh} regulates reduced flavin transfer to its linked bacterial luciferase (only the monomeric enzyme binds to luciferase) (*22*). However, unlike FRP_{Vh} and FRG_{Vf}, which each contains a tightly bound FMN cofactor in a 1:1 monomeric ratio and uses a ping-pong kinetic mechanism, FRD_{Aa} is unusual because it also has an FMN cofactor but in a nonconstant ratio (typically, 1 FMN per dimer) and follows a sequential ordered kinetic mechanism (*8*). One fundamental difference is that FRD_{Aa} belongs to a different flavin reductase subfamily (CDD ID: pfam01613) than FRP_{Vh} and FRG_{Vf}, and this subfamily of enzymes shows greater diversity among its sequences, molecular masses, and quaternary structures than enzymes from luminous bacteria and *E. coli*.

The homology of the FRD_{Aa} flavin reductase subfamily is found within the conserved flavin reductase domain, which is hypothesized to be the location of the active site (Figure 1). Within the flavin reductase domain is a near universally conserved GDH motif, which is believed to be the primary determinant of the pyridine nucleotide interaction with each enzyme (*23*). Because both the crystal structures and data for which residues determine pyridine nucleotide specificity in FRP_{Vh} and FRG_{Vf} are available (*13*, *17*, *24*), this study aimed to extend our knowledge of FRD_{Aa} by establishing which residues are responsible for pyridine nucleotide specificity in this NADH-specific enzyme. Histidine is often a functional residue; therefore, the highly conserved His140 in the GDH motif was targeted for analysis in this study. An H140A mutant demonstrated <3% of normal enzyme activity even with high concentrations of substrate and enzyme. Anaerobic stopped-flow measurements established that H140A FRD_{Aa} did retain catalytic activity, but it was markedly reduced compared to the wild-type enzyme and with no apparent saturation. These data suggest that His140 is indeed critical for the interaction and binding of NADH to the enzyme active site and is important to the hydride transfer from NADH to the bound FMN cofactor. This is the first known study identifying a critical active-site residue in the NADH-specific class of flavin reductases.

EXPERIMENTAL PROCEDURES

Materials. FMN and NADH were from Sigma. IPTG, dithiothreitol, and the *E. coli* JM109 competent cells were from Promega. Oligonucleotide primers were from MWG Biotech. Ultrafiltration membranes were from Millipore. DEAE Cellulose DE-52 was from Whatman. DEAE Sepharose resin and the HiLoad16/60 Superdex 200-pg column were from Amersham. The Bradford protein concentration reagents were from Bio-Rad. Unless otherwise stated, phosphate (P_i) buffers consisted of mole fractions of 0.39 sodium monobase and 0.61 potassium dibase in deionized water with the pH adjusted to 7.8 using aliquots of 5 M NaOH.

Site-Directed Mutagenesis. Mutagenesis of wild-type frd_{Aa} was performed using the Stratagene QuikChange site-directed mutagenesis kit according to the directions from the manufacturer. A variation from the protocol was that the mutant DNA was directly used to transform *E. coli* JM109 competent cells instead of the XL-1 Blue Supercompetent cells supplied with the kit. The dsDNA template was plasmid $pFRD_{Aa}$ (*8*). The codon CAT encoding His140 was changed to GCT to obtain Ala140. The alanine mutation was verified (plasmid name: $pH140AFRD_{Aa}$) through sequencing performed at Lone Star Labs (Houston, TX).

Enzyme Purification. The wild-type and mutant FRD_{Aa} enzymes were each purified according to a previously published protocol (*8*) and were determined to be approximately 90% pure based upon analysis of an SDS−PAGE (*25*) gel image with SigmaGel gel-scanning software.

Preparation of the H140A FRD_{Aa} Apoenzyme. The apoenzyme was prepared with a guanidine·HCl/urea denaturation column and renatured by dilution into swirling P_i buffer using previously published methods (*12*, *16*).

Flavin Binding to H140 FRD_{Aa}. The FMN/dimeric H140A FRD_{Aa} ratio following purification of the native H140A FRD_{Aa} was determined by comparing the concentration of bound FMN (determined spectrophotometrically at 455 nm using a molar absorption coefficient of 1.25×10^4 M^{-1} cm^{-1}) to protein. The FMN/dimeric H140A FRD_{Aa} ratio was also determined following saturation with FMN using ultrafiltration (*4*) with a 30000 MWCO poly(ether sulfone) membrane. The stoichiometry and K_d of FMN binding to the apoenzyme of H140A FRD_{Aa} were also determined by fluorescence quenching of the enzyme upon FMN titration. Excitation was set at 295 nm, and emission was monitored at 330 nm using a Varian Cary Eclipse fluorescence spectrophotometer. Inner filter effects on excitation and emission because of high concentrations of FMN were corrected using the relationship (*26*)

$$F_{\text{corrected}} = F_{\text{observed}} \times 10^{-0.5 l_{\text{ex}} A_{\text{ex}}} \times 10^{-0.5 l_{\text{em}} A_{\text{em}}} \quad (3)$$

where l_{ex} and l_{em} are, respectively, the cuvette full-path length (cm) along the direction of excitation and emission light and A_{ex} and A_{em} are, respectively, the absorbance of the sample (at a 1-cm light path) at the excitation and emission wavelength settings.

Optical Spectroscopy. Absorption spectra and absorbance measurements at a desired wavelength were obtained by using a Varian Cary 50 Bio UV−vis spectrophotometer. Circular dichroism (CD) spectra were measured at 23 °C using an Olis DSM 1000 CD spectrophotometer. Stopped-flow spectroscopy was performed at 23 °C using an Olis rapid scanning monochromator. For stopped-flow spectroscopy, enzyme and NADH solutions at designated concentrations were made anaerobic with glucose oxidase present at 2% of the concentration of the enzyme and 1 mM glucose and by gently blowing ultrahigh purity nitrogen gas into glass syringes for 2 h. The syringes were sealed and transferred to a glovebox containing the stopped-flow apparatus, which was flushed with nitrogen gas for the duration of the experiment. Reactions were initiated by mixing 125 μL of solution 1 with an equal volume of solution 2. The absorption spectra of the mixed solution was scanned in the range of 349−577 nm, and reduction of FMN was confirmed by monitoring the decrease of the flavin absorption at 455 nm. Depending on the length of the assay, scans were collected at the rate of 21, 31, 62, or 1000 s^{-1}.

Spectrophotometer Assays. Flavin reductase activity under standard assay conditions was measured at 23 °C by monitoring the A_{340} decrease associated with the oxidation of NADH in a 1-cm light path. All reactions were initiated by adding NADH into 1 mL of 50 mM P_i containing 1 μM FRD_{Aa} or H140A FRD_{Aa} (calculated using a monomer molecular mass of 34.5 kDa) and a designated concentration of FMN. The concentrations of NADH were determined from A_{340} measurements using $\epsilon_{340} = 6.22 \times 10^3$ M^{-1} cm^{-1}.

Protein Concentration. Concentrations of FRD_{Aa} and H140A FRD_{Aa} were determined by the method of Bradford (*27*) with bovine serum albumin as a standard.

Computer Analyses. Protein sequence similarity searches were performed using BLASTP (*28*) on the NCBI server (http://www.ncbi.nlm.nih.gov/BLAST/). The flavin reductase domain consensus sequence (CDD ID: pfam01613.11, Flavin_Reduct) was accessed via CDD (*29*, *30*) also on the NCBI server. Multiple sequence alignments were made with CLUSTALW (*31*) on the Baylor College of Medicine−Human Genome Science Center server (http://searchlauncher-.bcm.tmc.edu/multi-align/multi-align.html) (*32*). The X-ray diffraction structure of *Archaeoglobus fulgidus* FeR (PDB ID: 1I0R) was accessed on the PDB server (http://www.pdb.org/) (*33*).

RESULTS

Site-Directed Mutagenesis of FRD_{Aa}. Wild-type FRD_{Aa} was successfully mutated to H140A FRD_{Aa}, and expression yields ranged between 50 and 150 mg but were typically ∼75 mg per 12 L of culture. Such yields were actually better than that of the wild-type enzyme (∼35 mg per 12 L, using an identical expression and purification protocol). CD spectra of the wild-type and H140A FRD_{Aa} were measured and compared in the range of 190−260 nm. Both samples exhibited essentially identical spectra, indicating that the H140A mutation did not result in any significant conformational change.

Under standard assay conditions, H140A FRD_{Aa} exhibited a marginally measurable apparent activity, which was at best <3% of the activity of the wild-type enzyme, using 320 μM NADH and 2.5 μM FMN. A similar level of activity can be obtained with the same concentrations of NADH and free FMN in the absence of the enzyme. At 320 μM NADH, increases of the H140A FRD_{Aa} concentration from 1 to 10 μM or increases of the FMN concentration from 2.5 to 20 μM did not result in any significant increases in the observed NADH oxidation rates. These results indicate that the true catalytic activity of H140A FRD_{Aa}, if any, must be very low and cannot be accurately measured by the standard spectrophotometric assay.

Flavin Binding to H140A FRD_{Aa}. After purification, a fixed concentration of H140A FRD_{Aa} was found to contain less bound FMN than an identical concentration of the wild-type enzyme (the ratio was somewhat variable but typically at 1 FMN per 8 mutant enzyme monomers). To test whether H140A FRD_{Aa} is similar to the wild-type enzyme, which is capable of binding one FMN cofactor per monomer, 45 μM FMN was added to a 10 μM aliquot of H140A FRD_{Aa} containing 1.4 μM bound FMN and the mixture was incubated for 15 min. The sample volume was halved in an ultrafiltration cell, and the concentrations of H140A FRD_{Aa} and FMN were determined for both the retentate and filtrate. The concentration of H140A FRD_{Aa} in the retentate increased from 10 to 20 μM. The total concentration of FMN in the enzyme sample before filtration was 46.4 μM (45 μM free FMN + 1.4 μM bound FMN), which increased to 57 μM FMN in the retentate following filtration. Free FMN in the filtrate was 35 μM after filtration. Thus, the final concentration of H140A FRD_{Aa}-bound FMN was 22 μM. Because the final concentration of H140A FRD_{Aa} was 20 μM, this indicates the binding of 1 FMN per H140A FRD_{Aa} monomer. This ratio is identical to that of the wild-type enzyme.

Apoenzyme was obtained from the native H140A FRD_{Aa} following a denaturation−renaturation procedure (*12*, *16*), to reduce the FMN cofactor content to as low as 1% of the enzyme monomeric concentration. Because the quality of the apoenzyme sample cannot be assessed by the activity assay upon reconstitution with FMN, CD spectra of the apo- and holoenzyme forms of H140A FRD_{Aa} were compared in the 190−260 nm range. No significant differences were detected, indicating that no significant conformational change had occurred within the mutant apoenzyme after FMN cofactor removal. Using such a sample, the stoichiometry and K_d for FMN binding were determined by monitoring H140A FRD_{Aa} fluorescence quenching. First, 5 μM H140A apoFRD_{Aa} was titrated with various amounts of FMN. As shown in Figure 2A, sharp decreases of protein fluorescence were observed at increasing concentrations of FMN when the [FMN]/[monomeric apoenzyme] molar ratios were <1. The linear part of protein fluorescence quenching at lower FMN concentrations and the final protein fluorescence level obtained at high FMN concentrations intersect at a point corresponding closely to an [FMN]/[monomeric apoenzyme] molar ratio of 1. This finding is consistent to and reinforces the 1:1 binding of FMN cofactor by monomeric H140A FRD_{Aa} shown by the ultrafiltration measurements.

Additionally, a limiting amount (0.2 μM) of H140A apoFRD_{Aa} was titrated with increasing levels of FMN, and changes in H140A apoFRD_{Aa} fluorescence (Δ(fluorescence) defined as the fluorescence of H140A apoFRD_{Aa} without any addition of FMN minus that after the addition of a designated level of FMN) were determined. A double-reciprocal plot of Δ(fluorescence) versus the concentration of added FMN

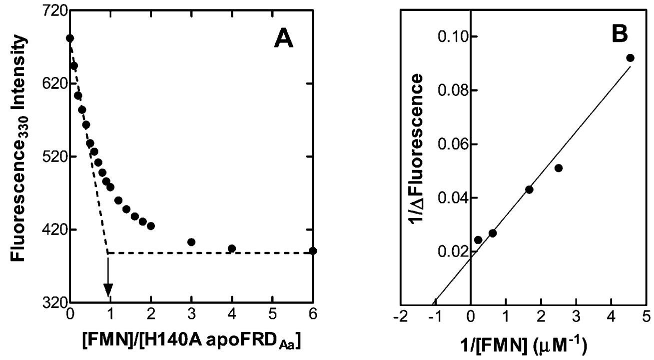

FIGURE 2: Fluorometric titrations of H140A apoFRD_{Aa} with FMN. (A) Constant amount of H140A apoFRD_{Aa} at 5 μM monomeric concentration was titrated with FMN in 50 mM P_i at various molar ratios as indicated. Emission intensities at 330 nm were measured using an excitation at 295 nm and are plotted against the molar ratio of [FMN]/[H140A apoFRD_{Aa}]. For samples containing $\geq$3 μM FMN, observed H140A apoFRD_{Aa} fluorescence intensities were corrected for the inner-filter effects of FMN on both excitation and emission as described in the Experimental Procedures. (B) H140A apoFRD_{Aa} at 0.2 μM was titrated with several levels of FMN as indicated. After incubation for 5 min at each concentration, fluorescence intensities at 330 nm were measured using an excitation at 300 nm. Δ(Fluorescence) is defined as the emission intensity of H140A apoFRD_{Aa} minus that with the designated concentration of FMN. Data are shown as a double-reciprocal plot.

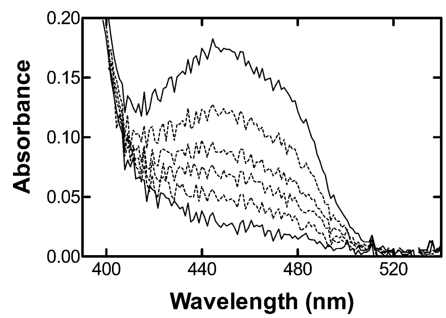

FIGURE 3: Anaerobic reduction of H140A FRD_{Aa} by NADH. Equal volumes of an FRD_{Aa} sample containing 13.2 μM bound FMN and an NADH (5.6 mM) solution, both in 50 mM P_i at pH 7.8, were mixed at 23 °C in a rapid-scanning stopped-flow spectrophotometer under anaerobic conditions as described under the Experimental Procedures. The time-dependent absorption spectral changes were measured in the 400−535 nm range. Spectra shown here, from top to bottom, are those taken at 0, 11, 22, 30, 44, and 70 s after mixing.

gives a linear line (Figure 2B), and a K_d of 0.9 μM was obtained from the abscissa intercept.

Anaerobic Stopped-Flow Measurements of Wild-Type and H140A FRD_{Aa}. The bound FMN cofactor of the native FRD_{Aa} can be fully reduced anaerobically by NADH (*8*). Although much slower in rate, the bound FMN of H140A FRD_{Aa} can also be fully reduced by NADH as shown by stopped-flow anaerobic measurements (Figure 3). Kinetics of reductions of both of the native and H140A FRD_{Aa} by NADH were determined by following the time courses of ΔA_{455} (associated with the bleaching of the bound FMN cofactor) using a fixed amount of enzyme and varying levels of NADH. When NADH levels were in excess to the enzyme concentration, the reductions of the FMN cofactor bound to either enzyme closely followed apparent first-order kinetics. As an example, the time course of ΔA_{455} for the reduction of H140A FRD_{Aa} by 1.75 mM NADH is shown in Figure 4. The corresponding semilog plot is shown as the inset, showing a good linearity (goodness of fit r^2 = 0.985) as

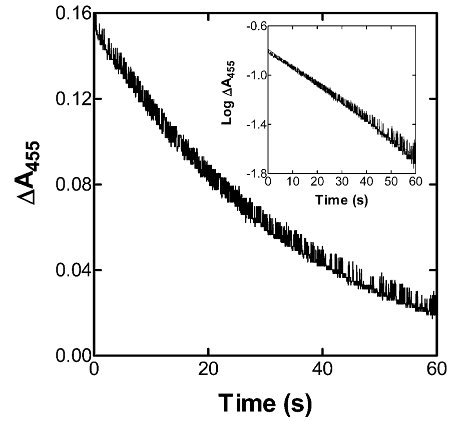

FIGURE 4: Kinetics of H140A FRD$_{Aa}$ reduction by NADH. Changes of absorbance at 455 nm upon anaerobic reduction of H140A FRD$_{Aa}$ with 1.75 mM NADH (final concentration) were measured under conditions similar to that described under the Experimental Procedures, and the time course of ΔA_{455} (defined as the absorbance observed at any given time minus the final sample absorbance upon completion of reduction) is shown. The same data set is replotted as log ΔA_{455} versus time in the inset.

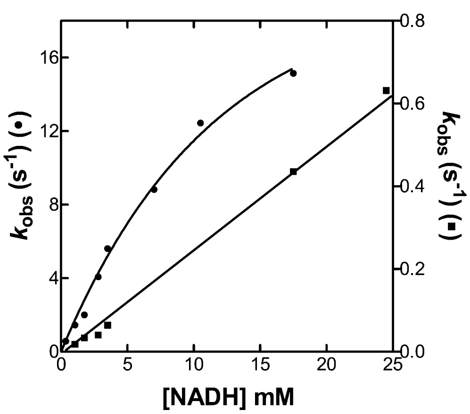

FIGURE 5: Dependence of the rate of FRD$_{Aa}$ reduction on the NADH concentration. Wild-type FRD$_{Aa}$ at 138 μM with 57.3 μM bound FMN (●) and 115 μM H140A FRD$_{Aa}$ with 13.2 μM bound FMN (■) were each reduced anaerobically with varying levels of NADH in a stopped-flow spectrophotometer. Pseudo-first-order rate constants (k_{obs}) of reduction were determined from plots of log ΔA_{455} versus time as described for the inset of Figure 4 and are shown here as a function of the NADH concentration immediately after mixing.

expected for an apparent first-order process. In this case, a k_{obs} of 0.033 s^{-1} was obtained. Values of k_{obs} for FMN cofactor reductions were determined similarly for both the native enzyme and H140A FRD$_{Aa}$ and are shown as a function of the NADH concentration used for reduction (Figure 5). While a saturation curve was obtained for the native FRD$_{Aa}$, a linear plot was observed for the mutant enzyme.

For the wild-type enzyme, the stopped-flow data can be analyzed according to the following reaction:

$$\text{E:FMN} + \text{NADH} \underset{k_2}{\overset{k_1}{\rightleftharpoons}} \text{E:FMN:NADH} \xrightarrow{k_3} \text{E:FMN}_2 + \text{NAD}^+ \quad (4)$$

in which E:FMN is the holoenzyme, the total concentration of NADH is in excess of the enzyme and cofactor FMN, and a fast equilibrium exists for the binding step (i.e., k_1 and $k_2 \gg k_3$). The model predicts a saturation curve of the observed rate constant (k_{obs}) versus the NADH concentration, and a linear double-reciprocal plot of k_{obs} versus the NADH concentration follows the relationship

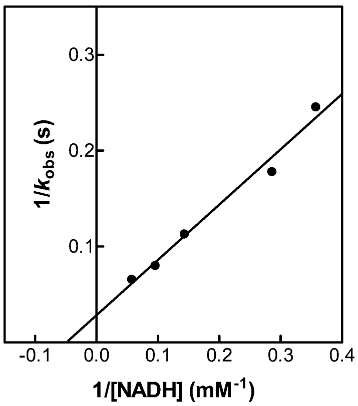

FIGURE 6: Double-reciprocal plot of k_{obs} of the wild-type FRD$_{Aa}$ anaerobic reduction versus the NADH concentration. Data are taken from that shown in Figure 6 for the wild-type enzyme.

$$\frac{1}{k_{obs}} = \frac{1}{k_3} + \frac{K_d}{k_3}\frac{1}{[\text{NADH}]} \quad (5)$$

where $K_d = k_2/k_1$ is the dissociation constant for NADH binding to FRD$_{Aa}$ holoenzyme. The double-reciprocal plot of k_{obs} versus [NADH] for FRD$_{Aa}$ using data from the curved part of the plot in Figure 5 (with [NADH] $\geq$ 2.8 mM) is shown in Figure 6. A linear relationship was obtained, allowing for the calculation of $k_3 = 34.5$ s^{-1} and $K_d = 20$ mM.

In a sharp contrast, the k_{obs} versus [NADH] plot for H140A FRD$_{Aa}$ shows a linear relationship up to 24.5 mM NADH. Moreover, the linear plot goes through the origin of the coordinates (Figure 5). Such characteristics are consistent with the following equation:

$$\text{E:FMN} + \text{NADH} \xrightarrow{k} \text{E:FMNH}_2 + \text{NAD}^+ \quad (6)$$

The lack of any detectable intercept on the ordinate indicates that no significant E:FMN:NADH complex was formed up to 24.5 mM NADH. The slope of this plot gives rise to $k = 26$ s^{-1} M^{-1}. Using the linear part of the k_{obs} versus [NADH] plot in Figure 5 for the native enzyme (with [NADH] < 2.8 mM), a corresponding k can be calculated to be 1370 s^{-1} M^{-1}.

DISCUSSION

The current genomic sequencing efforts accompanied by powerful sequence-alignment algorithms and improved homology-modeling methods have made it possible to a high degree of accuracy to identify probable residues in the active site that are critical for substrate binding and/or catalysis. This study represents one such case, in which the His140 of *A. aminovorans* FRD$_{Aa}$ was hypothesized to be important for enzyme function based upon a sequence alignment. This His140 of FRD$_{Aa}$ is within the GDH motif, which is almost universally conserved among the subfamily of flavoproteins containing the flavin reductase domain identified as pfam01613 (Figure 1). Galán et al. have published a sequence alignment clearly demonstrating the conserved nature of the GDH motif, and they also speculated it might be involved with the NAD-

(P)H−enzyme interactions (*23*). In this study, the hypothesized functional roles of the FRD_{Aa} H140 residue were tested by characterizations of the H140A mutant enzyme.

Using up to 320 μM NADH, 20 μM FMN, and 10 μM enzyme, <3% activity was detected for H140A FRD_{Aa}. CD measurements indicated that no significant conformational change had occurred as a consequence of this mutation. Hence, the drastic activity reduction of the mutated enzyme indicates a critical role of the His140 residue in the expression of FRD_{Aa} activity. A series of studies were subsequently carried out to elucidate further the functional roles of this critical residue.

First, the possibility that weakened binding of the cofactor FMN was responsible for the loss of activity was considered when it was apparent that a lesser amount of the cofactor FMN was bound to purified H140A FRD_{Aa} than to the wild-type enzyme. The ultrafiltration-binding assay and fluorescence quenching data (Figure 2A) demonstrated that H140A FRD_{Aa} was able to bind FMN in the same 1:1 stoichiometric ratio as the wild-type enzyme using a saturating concentration of FMN. The mutation did have an effect on the binding affinity for the cofactor FMN because the K_d of the mutant enzyme is slightly weaker (0.9 μM) than that of the wild-type enzyme (0.6 μM) (*8*). The levels of FMN used in activity assays were saturating with respect to the flavin cofactor binding. Therefore, weakened binding of the FMN cofactor could not be the primary reason for the absence of activity.

The ability of FRD_{Aa} to bind the NADH substrate and the efficiency in the FMN cofactor reduction by NADH were subsequently investigated and compared for both the native and the mutated enzymes in a series of anaerobic stopped-flow studies. Similar to the native enzyme (*8*), the H140A FRD_{Aa} was also capable of reducing the FMN cofactor by NADH (Figure 3). As shown in Figure 4 and other similar measurements, both the native and H140A FRD_{Aa} exhibited apparent first-order kinetics in the reduction of FMN cofactor by NADH when the latter was present in excess. However, there are two major differences between the two forms of reductases (Figure 5). First, the rates of FMN cofactor reductions by the mutant enzyme were substantially slower than those by the native enzyme under similar reduction conditions. Second, the wild-type enzyme showed a linear relationship in the k_{obs} versus [NADH] plot at low NADH levels but exhibited a saturation type of relationship at higher concentrations of NADH. In contrast, the mutant enzyme showed a good linear k_{obs} versus [NADH] plot up to 24.5 mM of NADH tested in this study.

For the wild-type enzyme, results shown in Figure 5 were analyzed according to eqs 4 and 5. The K_d for the binding of NADH to the native holoenzyme was determined to be 20 mM, and the k_3 for cofactor reduction by the bound NADH was obtained as 34.5 s^{-1}. The V_{max} of the native enzyme was previously determined to be 8.4 μmol of NADH reduction min^{-1} (mg enzyme)$^{-1}$ (*8*). This corresponds to a k_{cat} of 4.8 s^{-1}. The k_3 is significantly but not drastically faster than the k_{cat}, indicating that the FMN cofactor reduction could be partially rate-limiting but is followed by at least one slower step in the catalytic pathway.

As for the H140A FRD_{Aa}, a linear plot of k_{obs} versus [NADH] was obtained up to 24.5 mM NADH with the line going through the origin (Figure 5). These characteristics are consistent with the relationship shown in eq 6, which does not involve any significant formation of the holoenzyme−NADH complex. These results clearly demonstrated an essential role of the His140 residue in the binding of the NADH substrate by this enzyme. Furthermore, the efficiency of this mutant enzyme in FMN cofactor reduction by NADH can be judged by the bimolecular rate constant of 26 s^{-1} M^{-1}, obtained from the slope of the linear k_{obs} versus [NADH] plot (Figure 5). At low NADH concentrations, a linear relationship was also obtained for the native enzyme in the k_{obs} versus [NADH] plot (Figure 5). The corresponding bimolecular rate of FMN cofactor reduction by NADH was calculated to be 1370 s^{-1} M^{-1} for the wild-type enzyme, 53 times faster than that of the H140A FRD_{Aa}. These findings indicate further that the His140 residue of FRD_{Aa} was also important to the efficiency of cofactor reduction by NADH. This study provides the first identification of essential roles of a histidine within the conserved GDH motif in NADH binding and cofactor reduction for FRD_{Aa}-homologous flavin reductases.

In the group of homologous proteins shown in Figure 1, the atomic structure is only known for the ferric reductase FeR (PDB ID: 1I0R) from the hyperthermophilic archaean, *A. fulgidus* (*34*). A successful homology model of the flavin reductase PheA2 (it is from the same subfamily of flavin reductases as FRD_{Aa} and has 42% identity and 54% similarity with the flavin reductase domain of FRD_{Aa}) from *Bacillus thermoglucosidasius* A7 modeled against FeR was recently published (*35*). The atomic structure of FRD_{Aa} has not been determined. The polypeptide chain of FRD_{Aa} is almost twice as long as that of FeR, but the 169-residue polypeptide chain of FeR has 24% identity and 46% similarity to the corresponding segment of the polypeptide chain in FRD_{Aa}. The atomic structure of FeR reveals a critical hydrogen bond between His126 (which is equivalent to His140 of FRD_{Aa}) and the bound NADH. If an in silico mutation to alanine is made using InsightII, NADH can still orient itself into the active site, but the methyl side chain of alanine cannot form a hydrogen bond with the nicotinamide ring. Interestingly, the structure of FeR also suggests a catalytic role of His126 in hydride transfer. These probable structure−function features of FeR provide an interesting comparison with our findings that the His140 of FRD_{Aa} was critical to the binding and the reduction of the FMN cofactor by NADH. It is possible that the hydrogen bond between the histidine in the conserved GDH motif and the nicotinamide ring might represent a common mode of interaction and binding applicable to all flavin reductases within the FRD_{Aa} subfamily of flavin reductases.

ACKNOWLEDGMENT

We thank Dr. Glen Legge for allowing us to use the circular spectropolarimeter. We also thank Samer Kabbara for technical assistance.

REFERENCES

1. Tu, S.-C. (2001) Reduced flavin: Donor and acceptor enzymes and mechanisms of channeling, *Antioxid. Redox Signaling 3*, 881−897.
2. Low, J. C., and Tu, S.-C. (2002) Functional roles of conserved residues in the unstructured loop of *Vibrio harveyi* bacterial luciferase, *Biochemistry 41*, 1724−1731.

3. Low, J. C., and Tu, S.-C. (2003) Energy transfer evidence for *in vitro* and *in vivo* complexes of *Vibrio harveyi* flavin reductase P and luciferase, *Photochem. Photobiol. 77*, 446−452.
4. Kendrew, S. G., Harding, S. E., Hopwood, D. A., and Marsh, E. N. (1995) Identification of a flavin:NADH oxidoreductase involved in the biosynthesis of actinorhodin. Purification and characterization of the recombinant enzyme, *J. Biol. Chem. 270*, 17339−17343.
5. Kendrew, S. G., Hopwood, D. A., and Marsh, E. N. (1997) Identification of a monooxygenase from *Streptomyces coelicolor* A3(2) involved in biosynthesis of actinorhodin: Purification and characterization of the recombinant enzyme, *J. Bacteriol. 179*, 4305−4310.
6. Xun, L. (1996) Purification and characterization of chlorophenol 4-monooxygenase from *Burkholderia cepacia* AC1100, *J. Bacteriol. 178*, 2645−2649.
7. Gisi, M. R., and Xun, L. (2003) Characterization of chlorophenol 4-monooxygenase (TftD) and NADH:flavin adenine dinucleotide oxidoreductase (TftC) of *Burkholderia cepacia* AC1100, *J. Bacteriol. 185*, 2786−2792.
8. Russell, T. R., Demeler, B., and Tu, S. C. (2004) Kinetic mechanism and quaternary structure of *Aminobacter aminovorans* NADH:flavin oxidoreductase: An unusual flavin reductase with bound flavin, *Biochemistry 43*, 1580−1590.
9. Gerlo, E., and Charlier, J. (1975) Identification of NADH-specific and NADPH-specific FMN reductases in *Beneckea harveyi*, *Eur. J. Biochem. 57*, 461−467.
10. Jablonski, E., and DeLuca, M. (1978) Studies of the control of luminescence in *Beneckea harveyi*: Properties of the NADH and NADPH:FMN oxidoreductases, *Biochemistry 17*, 672−678.
11. Lei, B., Liu, M., Huang, S., and Tu, S.-C. (1994) *Vibrio harveyi* NADPH−flavin oxidoreductase: Cloning, sequencing, and overexpression of the gene and purification and characterization of the cloned enzyme, *J. Bacteriol. 176*, 3552−3558.
12. Liu, M., Lei, B., Ding, Q., Lee, J. C., and Tu, S.-C. (1997) *Vibrio harveyi* NADPH:FMN oxidoreductase: Preparation and characterization of the apoenzyme and monomer−dimer equilibrium, *Arch. Biochem. Biophys. 337*, 89−95.
13. Tanner, J. J., Lei, B., Tu, S.-C., and Krause, K. L. (1996) Flavin reductase P: Structure of a dimeric enzyme that reduces flavin, *Biochemistry 35*, 13531−13539.
14. Inouye, S. (1994) NAD(P)H−flavin oxidoreductase from the bioluminescent bacterium, *Vibrio fischeri* ATCC 7744, is a flavoprotein, *FEBS Lett. 347*, 163−168.
15. Zenno, S., Saigo, K., Kanoh, H., and Inouye, S. (1994) Identification of the gene encoding the major NAD(P)H−flavin oxidoreductase of the bioluminescent bacterium *Vibrio fischeri* ATCC 7744, *J. Bacteriol. 176*, 3536−3543.
16. Tang, C. K., Jeffers, C. E., Nichols, J. C., and Tu, S.-C. (2001) Flavin specificity and subunit interaction of *Vibrio fischeri* general NAD(P)H−flavin oxidoreductase FRG/FRase I, *Arch. Biochem. Biophys. 392*, 110−116.
17. Koike, H., Sasaki, H., Kobori, T., Zenno, S., Saigo, K., Murphy, M. E., Adman, E. T., and Tanokura, M. (1998) 1.8 Å crystal structure of the major NAD(P)H:FMN oxidoreductase of a bioluminescent bacterium, *Vibrio fischeri*: Overall structure, cofactor and substrate-analog binding, and comparison with related flavoproteins, *J. Mol. Biol. 280*, 259−273.
18. Fieschi, F., Nivière, V., Frier, C., Décout, J.-L., and Fontecave, M. (1995) The mechanism and substrate specificity of the NADPH:flavin oxidoreductase from *Escherichia coli*, *J. Biol. Chem. 270*, 30392−30400.
19. Louie, T. M., Yang, H., Karnchanaphanurach, P., Xie, X. S., and Xun, L. (2002) FAD is a preferred substrate and an inhibitor of *Escherichia coli* general NAD(P)H:flavin oxidoreductase, *J. Biol. Chem. 277*, 39450−39455.
20. Filisetti, L., Fontecave, M., and Niviere, V. (2003) Mechanism and substrate specificity of the flavin reductase ActVB from *Streptomyces coelicolor*, *J. Biol. Chem. 278*, 296−303.
21. Bucheli-Witschel, M., and Egli, T. (2001) Environmental fate and microbial degradation of aminopolycarboxylic acids, *FEMS Microbiol. Rev. 25*, 69−106.
22. Jeffers, C. E., Nichols, J. C., and Tu, S.-C. (2003) Complex formation between *Vibrio harveyi* luciferase and monomeric NADPH:FMN oxidoreductase, *Biochemistry 42*, 529−534.
23. Galán, B., Díaz, E., Prieto, M. A., and García, J. L. (2000) Functional analysis of the small component of the 4-hydroxyphenylacetate 3-monooxygenase of *Escherichia coli* W: A prototype of a new flavin:NAD(P)H reductase subfamily, *J. Bacteriol. 182*, 627−636.
24. Wang, H., Lei, B., and Tu, S.-C. (2000) *Vibrio harveyi* NADPH−FMN oxidoreductase Arg203 as a critical residue for NADPH recognition and binding, *Biochemistry 39*, 7813−7819.
25. Ausubel, M. F. (1993) in *Current Protocols in Molecular Biology*, John Wiley and Sons: New York.
26. Tu, S.-C., and McCormick, D. B. (1974) Conformation of porcine D-amino acid oxidase as studied by protein fluorescence and optical rotatory dispersion, *Biochemistry 13*, 893−899.
27. Bradford, M. M. (1976) A rapid and sensitive method for the quantitation of microgram quantities of protein utilizing the principle of protein-dye binding, *Anal. Biochem. 72*, 248−254.
28. Altschul, S. F., Gish, W., Miller, W., Myers, E. W., and Lipman, D. J. (1990) Basic Local Alignment Search Tool, *J. Mol. Biol. 215*, 403−410.
29. Marchler-Bauer, A., Panchenko, A. R., Shoemaker, B. A., Thiessen, P. A., Geer, L. Y., and Bryant, S. H. (2002) CDD: A database of conserved domain alignments with links to domain three-dimensional structure, *Nucleic Acids Res. 30*, 281−283.
30. Marchler-Bauer, A., Anderson, J. B., DeWeese-Scott, C., Fedorova, N. D., Geer, L. Y., He, S., Hurwitz, D. I., Jackson, J. D., Jacobs, A. R., Lanczycki, C. J., Liebert, C. A., Liu, C., Madej, T., Marchler, G. H., Mazumder, R., Nikolskaya, A. N., Panchenko, A. R., Rao, B. S., Shoemaker, B. A., Simonyan, V., Song, J. S., Thiessen, P. A., Vasudevan, S., Wang, Y., Yamashita, R. A., Yin, J. J., and Bryant, S. H. (2003) CDD: A curated Entrez database of conserved domain alignments, *Nucleic Acids Res. 31*, 383−387.
31. Thompson, J. D., Higgins, D. G., and Gibson, T. J. (1994) CLUSTAL W: Improving the sensitivity of progressive multiple sequence alignment through sequence weighting position-specific gap penalties and weight matrix choice, *Nucleic Acids Res. 22*, 4673−4680.
32. Smith, R. F., Wiese, B. A., Wojzynski, M. K., Davison, D. B., and Worley, K. C. (1996) BCM search launcher−An integrated interface to molecular biology database search and analysis services available on the World Wide Web, *Genome Res. 6*, 454−462.
33. Berman, H. M., Westbrook, J., Feng, Z., Gilliland, G., Bhat, T. N., Weissig, H., Shindyalov, I. N., and Bourne, P. E. (2000) The Protein Data Bank, *Nucleic Acids Res. 28*, 235−242.
34. Chiu, H. J., Johnson, E., Schroder, I., and Rees, D. C. (2001) Crystal structures of a novel ferric reductase from the hyperthermophilic archaeon *Archaeoglobus fulgidus* and its complex with $NADP^+$, *Structure 9*, 311−319.
35. Kirchner, U., Westphal, A. H., Muller, R., and van Berkel, W. J. (2003) Phenol hydroxylase from *Bacillus thermoglucosidasius* A7, a two-protein component monooxygenase with a dual role for FAD, *J. Biol. Chem. 278*, 47545−47553.

BI048499N